# Quiet New Particle Formation is a significant aerosol source in the Amazon boundary layer

Bruno B. Meller[1,3], Marco A. Franco[2], Rafael Valiati[1], Christopher Pöhlker[3], Luiz A. T. Machado[1,3], Florian Ditas[3,a], Leslie A. Kremper[3,a], Subha S. Raj[3], Cleo Q. Dias-Júnior[4,5], Flávio A. F. D'Oliveira[5], Luciana V. Rizzo[1], Ulrich Pöschl[3], and Paulo Artaxo[1,6]

[1]Institute of Physics, University of São Paulo, São Paulo, SP, 05508-900, Brazil.
[2]Department of Atmospheric Sciences, Institute of Astronomy, Geophysics and Atmospheric Sciences, University of São Paulo, São Paulo, SP, 05508-900, Brazil.
[3]Multiphase Chemistry Department, Max Planck Institute for Chemistry, 55128 Mainz, Germany.
[4]National Institute of Amazonian Research (INPA-CLIAMB), Manaus, AM, 69060-001, Brazil.
[5]Department of Physics, Federal Institute of Pará (IFPA), Belém, PA, 66093-020, Brazil.
[6]Center for Sustainable Amazon Studies (CEAS), University of São Paulo, São Paulo, Brazil
[a]now at: Hessian Agency for Nature Conservation, Environment and Geology, 65203 Wiesbaden, Germany.

*Correspondence to*: Paulo Artaxo (artaxo@if.usp.br)

**Abstract.** Aerosol particles formed by new particle formation (NPF) are essential for cloud condensation nuclei and can strongly influence cloud properties and climate. However, the mechanisms behind NPF in the Amazon boundary layer have remained elusive. Classical "banana" NPF events, common in other continental regions, are rarely observed in the Amazon, while most detected sub-50 nm particles have been linked to precipitation- and downdraft-related episodes, often called Amazonian banana events. Here, we analyse a decade of particle number size distributions (10–420 nm) from the Amazon Tall Tower Observatory (ATTO) during the wet season and demonstrate the presence of a distinct phenomenon called Quiet NPF. This process represents a subtle but persistent background particle formation, occurring on days without clear banana-type growth signatures. Using a statistical approach, we show that Quiet NPF links freshly formed 10 nm particles to growth into the Aitken mode. This mechanism is characterized by a growth rate of $2.4 \pm 0.1$ nm $h^{-1}$, about half that of Amazonian banana events, but occurs much more frequently. Quiet NPF accounts for ~45% of 10–25 nm particle production during the wet season, revealing an overlooked but important source of nanoparticles that contributes to sustaining Amazonian aerosol populations.

## 1 Introduction

New Particle Formation (NPF) contributes to atmospheric aerosols globally, influencing cloud condensation nuclei (CCN) and the climate (Spracklen et al., 2008; Gordon et al., 2017). Typically identified by a distinct "banana" shape in particle number size distribution (PNSD) plots, classical NPF events involve the nucleation of particles at ~1–3 nm and subsequent growth (Dal Maso et al., 2005; Kulmala et al., 2013; Dada et al., 2018). Recent studies revealed continuous but subtle aerosol formation, termed "Quiet NPF," occurring on days classified as non-event days due to the absence of clear nucleation

and growth signatures (Kulmala et al., 2022a, 2024). Thus, focusing only on NPF events biases studies toward intense cases. This quiet mechanism can substantially contribute to particle numbers annually, particularly where classical NPF events are infrequent (Kulmala et al., 2022a).

In Amazonia's wet season, aerosol composition is characterized by a prevalence of biogenic secondary organic aerosols (SOA) resulting from volatile organic compound (VOC) oxidation (Pöschl et al., 2010; Artaxo et al., 2013, 2022; Chen et al., 2015), though occasional intrusions of long-range transported African aerosols occur (Valiati et al., 2025). However, classical NPF events, as observed in boreal or mid-latitude regions, are notably absent in the Amazon boundary layer (BL). Instead, observational studies in the BL typically find only sparse regional NPF events, with most sub-50 nm particles linked to convective downdrafts that transport particles from aloft (Rizzo et al., 2018; Machado et al., 2021; Franco et al., 2022, 2024). New particle formation at low heights has therefore been primarily attributed to vertical transport from upper-tropospheric nucleation (Martin et al., 2010; Wang et al., 2016; Andreae et al., 2018; Zhao et al., 2022, 2024). Flight field observations, chamber studies, and box models have indicated that, in the Amazonian upper troposphere, isoprene oxidation generates highly oxygenated molecules (HOMs) — specifically extremely-low-volatility and ultra-low-volatility organic compounds (ELVOCs and ULVOCs) — driving substantial NPF (Curtius et al., 2024; Shen et al., 2024; Bardakov et al., 2024).

Nevertheless, uncertainty persists regarding BL aerosol formation. Recent studies highlight potential local and regional nucleation processes close to the canopy, driven by rainfall events and challenging existing assumptions (Machado et al., 2024). Numerical simulations also indicate that the vertical transport of newly nucleated ultrafine particles from the upper troposphere to the BL is inefficient on time scales of a few days (Wang et al., 2023). Crucially, the chemical mechanisms controlling these local processes remain poorly characterized, with ongoing debates surrounding the roles of isoprene, monoterpenes, and sesquiterpenes (Heinritzi et al., 2020; Dada et al., 2023).

In this study, we analyzed a decade-long (2014-2023) record of aerosol size distributions from the Amazon Tall Tower Observatory (ATTO) during its wet season (January – May), when the atmosphere best reflects natural background conditions. Using a novel statistical approach (Kulmala et al., 2022a), we demonstrate the presence and significance of Quiet NPF in the Amazon BL, characterising its unique formation and growth dynamics and quantifying its contribution to sub-50 nm aerosol populations.

## 2 The Characteristics and Relevance of Quiet NPF in the Amazon

### 2.1 Identification of Quiet NPF through Diurnal Dynamics of Particle Size Distributions

This study identifies and characterizes Quiet NPF during non-event days within the Central Amazon BL during its wet season. Quiet NPF differs from both classical NPF events—high formation rate episodes rarely observed in the Amazon—and from the more frequent "Amazonian bananas" (i.e., rainfall/downdraft-related events, with lower particle concentrations and higher initial diameters). Both classical events and Amazonian bananas exhibit clear, banana-shaped features in PNSDs.

In contrast, Quiet NPF is a subtle and persistent process that lacks such distinct signatures. By examining median diurnal cycles from extensive datasets, we reduce noise and ambient inhomogeneities effects, revealing the typical behaviour and daily growth dynamics of Quiet NPF in this environment.

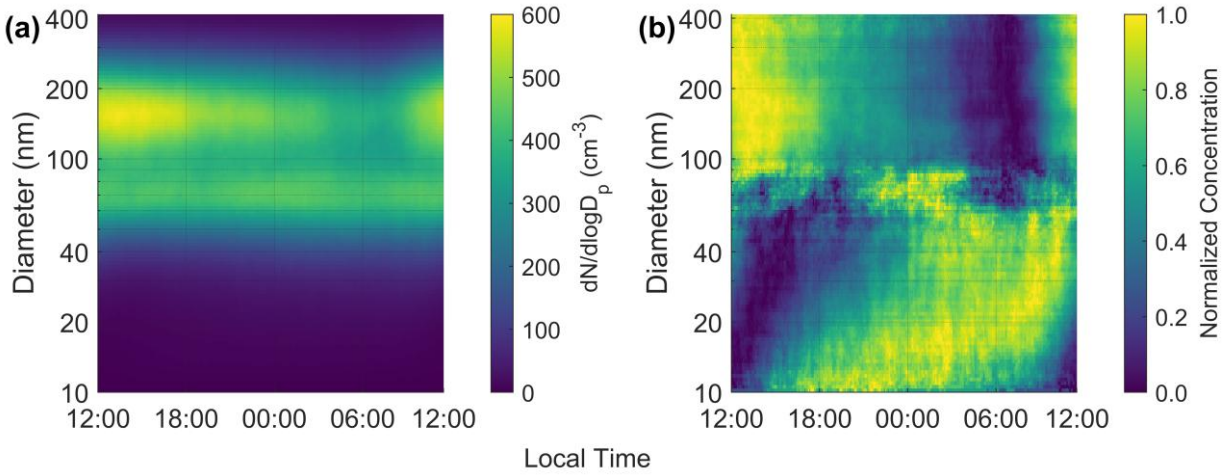


**Figure 1. Median diurnal cycle of the (a) absolute and (b) normalized particle number size distribution during non-event days at the Amazon Tall Tower Observatory (ATTO) from 2014 to 2023 during the wet season. Panel (a) does not show visible particle growth, emphasising the subtle nature of Quiet NPF. Panel (b) enhances the visibility of particle growth by normalizing concentrations in each diameter bin, clearly illustrating slow, sequential particle growth from around 10 nm to Aitken-mode size, characteristic of Quiet NPF.**

**Figure 1** illustrates the median diurnal cycle of the (a) absolute and (b) normalized PNSD observed during non-event days at ATTO. The absolute PNSD (**Fig. 1a**) primarily shows the dynamics of accumulation and Aitken-mode particles, which are influenced by BL processes such as nocturnal deposition and daytime turbulent mixing. Notably, this panel does not reveal clear particle growth, showing the subtlety of Quiet NPF, which is obscured by the dominance of larger particle modes.

In contrast, the normalized PNSD shown in Fig. 1b presents daily maxima and minima for each diameter bin, scaled independently from 0 to 1. Accumulation mode particles exhibit relatively homogeneous diurnal behaviour, reflecting their common response to variations in boundary-layer height, which are expected to affect particle concentrations in a largely size-independent or only weakly size-dependent manner within a given mode. In comparison, the normalized PNSD for the smaller particles (diameter < 50 nm) exhibits a progressive, size-resolved temporal shift that cannot be explained by dilution or vertical mixing alone, with ~10 nm particles peaking at 18:00 followed by progressively larger peaks, culminating at ~60 nm by noon the next day.

A similar pattern was also observed in an independent analysis of the PNSD during the wet seasons of 2008–2014 at the nearby ZF2 site in the Central Amazon. Despite the coarser resolution, the data reveal an identical nocturnal growth pattern, with sub-50 nm particle concentrations peaking at night (**Fig. S1**). Together with additional sensitivity tests, this consistency strengthens the robustness of our interpretation. Specifically, screening for anthropogenic influence shows no systematic effect on the Quiet NPF signature (**Appendix D**), whereas analyses using different statistical aggregations indicate that the

same sequential increase in particle diameter (10-25 nm) persists across a wide range of concentration percentiles (**Appendix F**). Taken together, these independent lines of evidence indicate that Quiet NPF represents a general statistical property of non-event days in the Central Amazon, is not significantly affected by anthropogenic influence, and reflects particle formation processes that occur very frequently and become detectable only through detailed statistical normalization.

Meteorological analyses further elucidate Quiet NPF. Non-event days show predominantly positive median diurnal $\Delta\theta_e$ (**Fig. S2**), indicating a minimal influence from convective downdrafts. This supports a primarily BL-driven process for Quiet NPF, independent of upper tropospheric transport. In contrast, event days display the lowest negative $\Delta\theta_e$ values during the morning, coinciding with the highest precipitation frequency and aligning with known associations between Amazonian-banana events, precipitation, and convective downdrafts (Franco et al., 2022; Machado et al., 2024).

Interestingly, Aitken-mode particles within the 60–85 nm size range exhibit a distinct peak around midnight, unlike most other particle size ranges. This is potentially associated with nocturnal emissions of primary biogenic particles in the Aitken size range, as previously documented (Pöhlker et al., 2012; Rizzo et al., 2018; Glicker et al., 2019). This observation highlights the complexity of interactions between primary biogenic emissions and secondary aerosol formation processes occurring during the Quiet NPF process.

### 2.2 Growth and Formation Rates Associated with Quiet NPF

To characterize Quiet NPF, we derived a single characteristic GR by applying the appearance time method to the median PNSD of all non-event days within the 10–25 nm diameter range (Lehtipalo et al., 2014; Kulmala et al., 2022a). We identified the time when the particle concentration reached the closest to 50% of its maximum value within each diameter bin and applied linear regression to these time-diameter points to obtain the GR, as shown in **Fig. 2**. The resulting linear fit yielded a statistically significant GR of 2.4 ± 0.1 nm $h^{-1}$ ($R^2$ = 0.96, p-value < 0.01). This GR is lower compared to previously reported rates for classical growth events in the Amazon BL (4–6 nm $h^{-1}$; Rizzo et al., 2018; Franco et al., 2022) and on the lower range of the typical GR observed at continental sites worldwide (2–7 nm $h^{-1}$; Kerminen et al., 2018). Even when compared with lower nighttime GRs observed in the Amazon BL (4 nm $h^{-1}$; Franco et al., 2022), our obtained GR remains approximately twofold lower.

The following analysis assumes that Quiet NPF-related processes are virtually always present during non-event days, with varying intensity, as supported by the percentile-based analysis presented in **Appendix F**.

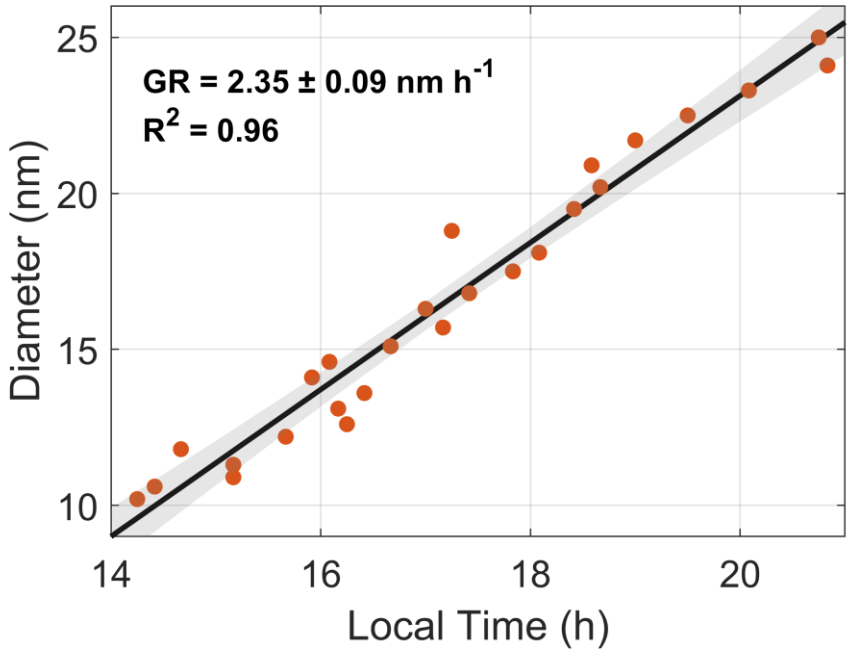


**Figure 2. Linear regression of particle growth rate (GR) using the appearance time method. Points represent the time when particle concentration in each diameter bin (10–25 nm) reached 50% of its daily maximum. The solid line indicates the statistically significant linear regression (GR = 2.35 ± 0.09 nm $h^{-1}$, p-value < 0.01), with the shaded area representing the 95% confidence interval.**

We subsequently calculated the formation rates of 10 nm particles ($J_{10}$) at 30-minute intervals on both event and non-event days, applying the aerosol population balance equation (Equation 1). The 10–25 nm diameter range encompasses particles that may be formed in the upper troposphere and transported to the BL. This vertical transport effect is known to influence event days significantly but is minimal on non-event days, consistent with predominantly positive $\Delta\theta_e$ values that indicate minimal downdraft contributions.

For event days, individual GR values were calculated per event, as indicated in Section 2. For non-event days, the obtained single representative GR value (2.4 nm $h^{-1}$) was uniformly applied. While this is a simplification — since growth rates could vary with precursor gas availability and properties (Kirkby et al., 2023) — the GR for non-event days can only be reliably obtained from long-term averages. Previous studies have shown that, despite substantial fluctuations in precursor concentrations, GR tends to vary only slightly within a given environmental condition (Kulmala et al., 2022b), which justifies this approach and aligns with the methodology of other studies (Kulmala et al., 2022a; Aliaga et al., 2023; Chen et al., 2023).

Using this approach, **Fig. 3a** and **3b** present the median diurnal cycles of $J_{10}$ for both event and non-event days, with individual contributions from each term in the balance equation explicitly shown. The *dN/dt* term reflects temporal variability in particle number, the "Coag." term accounts for particles lost to coagulation into larger particles (>25 nm), the

"Growth" term represents condensational growth, and "total" corresponds to $J_{10}$—the sum of all terms. As expected for Quiet NPF, $J_{10}$ during non-event days is substantially lower than during event days, in agreement with previous observations (Kulmala et al., 2022a). Notably, the coagulation term is proportionally larger on non-event days, indicating that slower growth rates increase the likelihood of newly formed particles being lost to coagulation. Because $J_{10}$ represents a net formation rate integrated over the 10–25 nm size range under slow-growth conditions, its diurnal maximum reflects cumulative growth and residence within this interval rather than the timing of the late-afternoon peak in 10 nm particle concentrations. In addition, dilution within a deeper, well-mixed BL during daytime likely contributes to reduced daytime $J_{10}$. Overall, the calculated formation rates for the Amazon are lower than those reported in other regions (Kirkby et al., 2023), consistent with the region's typically low concentrations of sub-50 nm particles.

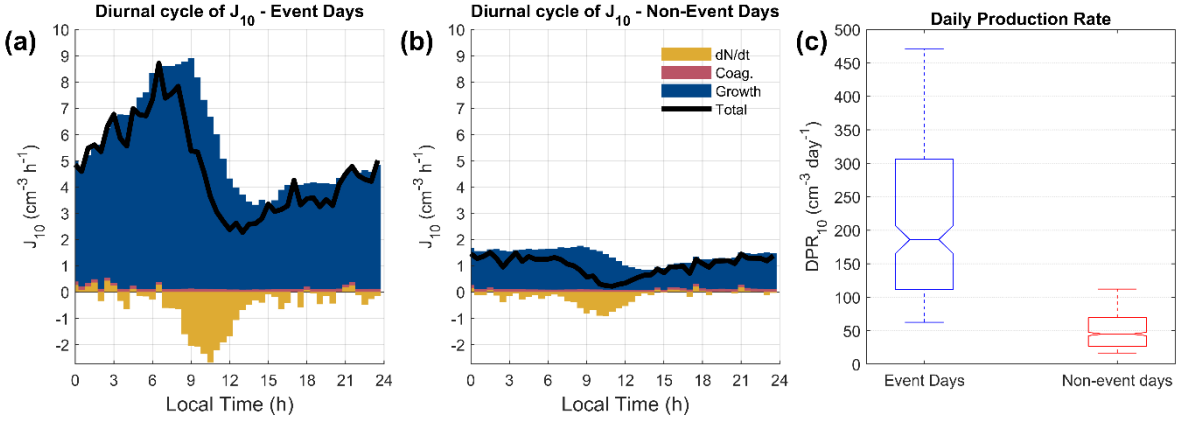


**Figure 3. Formation and production rates of 10 nm particles ($J_{10}$) during event and non-event days at ATTO. Panels (a) and (b) depict the median diurnal cycle of $J_{10}$ on event and non-event days, respectively, partitioned into individual terms from the aerosol balance equation: particle number concentration variation ($dN/dt$), coagulation sink (Coag.), and growth. Panel (c) compares daily production rates of particles (10–25 nm) for event (blue) and non-event (red) days. Boxes indicate the interquartile range (25th–75th percentiles), and whiskers represent the 10th and 90th percentiles.**

Integrating $J_{10}$ values over the entire day provided the daily particle production rates within the 10–25 nm range ($DPR_{10}$), presented in **Fig. 3c**. Median daily production rates (interquartile range) were 186 (111–309) $cm^{-3}$ $day^{-1}$ for event days and 45 (27–70) $cm^{-3}$ $day^{-1}$ for non-event days. For comparison, Kulmala et al. (2022a) reported a daily production rate of 286 $cm^{-3}$ $day^{-1}$ for particles between 6–25 nm during non-event days in Hyytiälä. Despite the narrower size range analyzed here, our observed lower production rates demonstrate the reduced particle formation capacity characteristic of the Amazonian BL.

Considering the higher frequency of non-event days (approximately 77%) compared to event days (23%), we estimate that Quiet NPF accounts for approximately 45% of the observed 10–25 nm particles during the wet season, highlighting its significant and persistent role in nanoparticle production in the Amazon BL. Although the absence of rain-related downdrafts and classical NPF events does not imply in principle that Quiet NPF is active on every non-event day, we use the median characteristics of non-event days to estimate its typical contribution. By examining additional percentiles, we find consistent

signatures across the distribution, supporting the applicability of this statistical approach to the full set of non-event days (see **Appendix F**). This approach is consistent with recent studies suggesting that new particle formation spans a continuum of intensities, from pronounced events to weaker, persistent processes (Kulmala et al., 2022a; Aliaga et al., 2023).

## 4 Discussions and conclusions

This study identified a previously unrecognized mechanism of new particle formation in the Amazon, termed Quiet NPF, which occurs in different locations within the Amazonian BL during the wet season. Our findings, in line with the proposal by Kulmala et al. (2024), demonstrate that NPF is not restricted to intense and easily identifiable growth episodes. By analysing a decade-long dataset of particle number size distributions and systematically aggregating days lacking clear nucleation signatures, we were able to characterize this subtle yet significant aerosol source. Quiet NPF fundamentally differs from the rainfall/downdraft-related events in the Amazon, as it is characterized by substantially lower growth rates (~2.4 nm $h^{-1}$) and particle formation rates (~1 $cm^{-3}$ $h^{-1}$). Nevertheless, due to its higher frequency, Quiet NPF makes a considerable contribution to the population of 10–25 nm particles, with an estimated daily production rate of approximately 45 $cm^{-3}$ $day^{-1}$. While this rate is lower than the 186 $cm^{-3}$ $day^{-1}$ observed during Amazonian banana event days, Quiet NPF accounts for roughly 45% of sub-25 nm particles during the wet season, highlighting its essential role in sustaining the Amazonian aerosol population.

A systematic difference is observed between downdraft-driven banana events, which predominantly occur during daytime, and Quiet NPF, for which $J_{10}$ exhibits higher and more sustained values during nighttime. This behaviour is consistent with lower accumulation-mode particle concentrations at night, which reduce the condensation and coagulation sinks, while daytime dilution within a deeper, well-mixed boundary layer likely contributes to lower $J_{10}$ values. The late-afternoon peak in ~10 nm particle concentrations suggests that the initial stage of Quiet NPF likely begins during daytime, whereas the slow growth rates imply weak condensational fluxes.

The pronounced differences in growth and formation rates, along with the temporal patterns distinguishing Quiet NPF from rainfall/downdraft-related events, point to distinct chemical mechanisms within the BL. Quiet NPF also differs from nucleation in the upper troposphere, where isoprene-derived organonitrates drive particle formation (Curtius et al., 2024; Zha et al., 2024). At ground-level temperatures, organonitrates formed from isoprene oxidation are not expected to contribute significantly to nucleation or the initial stages of particle growth (Heinritzi et al., 2020; Curtius et al., 2024). Moreover, ozone enhancements commonly observed during downdraft events (Machado et al., 2021, 2024) are unlikely to influence Quiet NPF, given the consistently lower ozone concentrations measured in the pristine Amazon BL during periods without downdrafts.

In summary, this study highlights a previously undocumented, frequent NPF mechanism within the Amazonian BL, distinct from nucleation and growth events associated with convective downdrafts and precipitation. Our findings underscore the complexity of aerosol dynamics in this unique environment and indicate that Quiet NPF represents a significant source of

newly formed particles, although its quantitative contribution to CCN-relevant sizes remains uncertain. While recent advances have improved our understanding of secondary aerosol production in the Amazon, our results suggest that this pathway may be underrepresented in current frameworks and merit further evaluation in both observations and models. Addressing this gap will require long-term measurements of sub-10 nm particles and detailed analyses of low-volatility precursor composition, enabling a more precise separation of the processes governing aerosol formation in the Amazon.

**Appendix A - Instrumentation and Data Processing**

This study was conducted at the ATTO site, situated in a remote, forested area of the Central Amazon, approximately 150 km northeast of Manaus, Brazil. This region is characterized by comparatively low aerosol concentrations during the wet season, making it an ideal natural laboratory to investigate the pristine aerosol life cycle (Artaxo et al., 2013, 2022). A comprehensive site description is available in Andreae et al. (2015). We analyzed a decade of measurements spanning 2014 to 2023, focusing exclusively on the wet season, defined as January to May.

Meteorological parameters, including pressure, temperature, relative humidity, and precipitation, were measured using a Barometer (PTB101, Vaisala), a Thermo-Hygrometer (IAK I-Series, Galltec-Mela), and a rain gauge (TB4, Hyquest Solutions) installed 81 m above ground level**.** To evaluate the influence of convective downdrafts on particle formation and/or transport, we calculated the potential equivalent temperature ($\theta_e$), a conservative thermodynamic variable that decreases with altitude. Sharp negative anomalies in $\theta_e$ are used to identify downdraft activity (Gerken et al., 2016; Dias-Junior et al., 2017). To remove the effect of diurnal variability, we calculated the diurnal anomaly of $\theta_e$, defined as the deviation of instantaneous $\theta_e$ from its median value at the same hour ($\Delta\theta_e$). Rather than directly identifying individual downdrafts, we used $\Delta\theta_e$ statistics to compare typical downdraft behaviour and frequency across different classes of days.

Black carbon (BC) concentrations were derived from long-term aerosol absorption measurements at ATTO. BC was primarily obtained from Multi-Angle Absorption Photometer (MAAP) measurements at 637 nm, following the site-specific calibration and correction procedures described by Saturno et al. (2018). Aethalometer (AE-33) data were used to fill occasional data gaps, with inter-instrument consistency validated as described by Franco et al. (2024).

Aerosol particle number size distributions (PNSD) were measured with Scanning Mobility Particle Sizers (SMPS; TSI classifiers 3080/3082 coupled with CPC models 3772/3750) placed inside the ATTO laboratory containers and sampling air through inlet lines from a height of 60 meters above ground, which corresponds to approximately 25 meters above the forest canopy. The SMPS provided online measurements of PNSD every 5 minutes for particle diameters ranging from 10.2 to 420 nm, with a 61% data coverage rate during wet seasons from 2014 to 2023. Detailed information on the design of the sample air inlet and dryer can be found elsewhere (Pöhlker et al., 2016).

To ensure data quality, measurements were corrected for diffusional, sedimentation, and inertial losses following Von der Weiden et al. (2009). The data were then smoothed using a two-dimensional mean filter, averaging over a 90-minute time

window and five diameter bins, as recommended by Kulmala et al. (2012). All concentrations were converted to standard temperature and pressure conditions (273.15 K, 1013.25 hPa) for consistency.

## Appendix B - Identification and characterization of growth events

Growth events were identified using criteria from Franco et al. (2022), which in turn are based on modifications to the method of Kulmala et al. (2012). Events were defined by the appearance of a distinct mode with a peak diameter between 10 and 40 nm, persisting for at least one hour, and exhibiting a positive shift in modal diameter. In comparison to "classical NPF events", this allows for the inclusion of "Amazonian Banana" episodes, where initial particle growth may not be local. Across the 2014–2023 wet seasons, 212 event days and 717 non-event days were identified, yielding a growth event frequency of 23%, consistent with Franco et al. (2022). Examples of both event and non-event days are shown in **Fig. B1**.

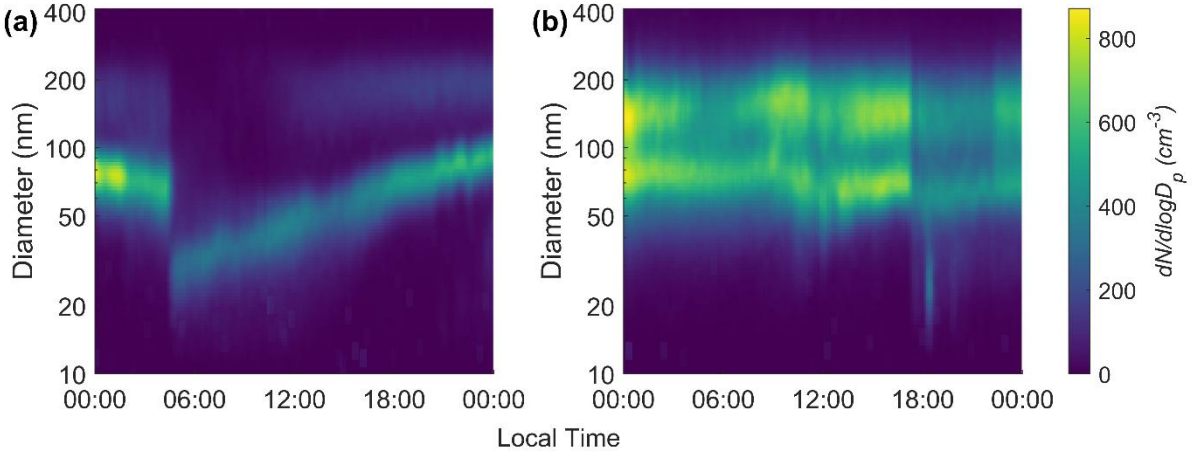


**Figure B1. Particle number size distribution during (a) a growth event day (09-Apr-2022) and (b) a non-event day (27-Apr-2022).**

For characterising events, we followed Franco et al. (2022), employing multi-lognormal fits to the PNSD, with three modes: sub-50 nm (10–50 nm), Aitken (50–100 nm), and accumulation (100–420 nm). Fits with $R^2 > 0.6$ and p-value < 0.05 were included. Growth rates (**GR**) for the events were calculated by linear regression of time versus geometric mean diameter in the sub-50 nm mode. Particle formation rates at 10 nm ($J_{10}$) were calculated using the aerosol population balance equation (Kulmala et al., 2012):

$$J_{10} = \frac{dN_{10-25}}{dt} + CoagS \times N_{10-25} + GR\left(\frac{dN}{dD_p}\right)_{25} \quad (1)$$

where $N_{10\text{-}25}$ is the concentration of particles in the 10–25 nm size range, $dN_{10\text{-}25}/dt$ is the time derivative representing the net temporal evolution of particle number concentration within this interval, $(dN/dD_p)_{25}$ is the particle number size distribution evaluated at 25 nm and represents the flux of particles growing out of the selected size range, and *CoagS* is the coagulation sink calculated from the size distribution using size-dependent coagulation coefficients (Kerminen et al., 2001; Seinfeld & Pandis, 2016). This formulation follows the aerosol population balance framework of Kulmala et al. (2012), in which the

formation rate $J_{10}$ is obtained by combining the observed temporal change in particle number with losses due to coagulation and condensational growth. The selected size range focuses the analysis on recently nucleated particles, minimizing contributions from primary sources.

**Appendix C - Analysis of Non-Event Days and Quiet NPF**

To better visualize sub-50 nm particle variability during non-event days, we calculated the diurnal median PNSD and normalized it using the method of Kulmala et al. (2022a), scaling each diameter bin's number concentration from 0 (minimum) to 1 (maximum) over the period of a day. This approach emphasises daily maxima and minima for each size class, regardless of absolute concentration, and highlights the evolution of particle populations even when absolute changes are subtle.

For the growth rate calculation on non-event days, the lognormal fit of the sub-50 nm mode was ill-defined due to low concentrations. Therefore, the appearance time method (Lehtipalo et al., 2014) was employed. Specifically, for diameters 10–25 nm, we identified the time each bin reached 50% of its daily maximum, then performed linear regression on these time-diameter pairs to estimate the GR. This method is well-suited for detecting gradual or subtle growth when lognormal fits are not applicable.

**Appendix D - Sensitivity analysis of Quiet NPF to anthropogenic influence**

Although the ATTO site is located in a remote region of the central Amazon, anthropogenic influence may occasionally reach the site via long-range or regional advection (Pöhlker et al., 2018; Holanda et al., 2023). Importantly, in the central Amazon, anthropogenic ultrafine particles transported over long distances typically have diameters larger than 10–25 nm. As a result, such contributions are not expected to produce the size-resolved growth signatures characteristic of Quiet NPF. Nevertheless, differences in the physical properties of the aerosol population could, in principle, affect the process characteristics. Given the weak intensity of Quiet NPF, even infrequent anthropogenic contributions could potentially bias the analysis if not explicitly evaluated.

To assess the robustness of our results with respect to anthropogenic influence, we conducted a sensitivity analysis using black carbon (BC) as a tracer. Following the aerosol population classification proposed by Valiati et al. (2025), we adopted a BC concentration of 0.064 μg $m^{-3}$ as an upper threshold representative of pristine aerosol conditions during the wet season at ATTO, when regional biogenic processes dominate aerosol properties. This threshold corresponds to the average BC concentration under pristine conditions and provides a conservative criterion while preserving sufficient data coverage for statistically meaningful analysis.

Using this criterion, we defined two datasets for comparison: (i) all non-event days during the wet season, and (ii) non-event days considering only 5-minute intervals with BC < 0.064 μg $m^{-3}$.

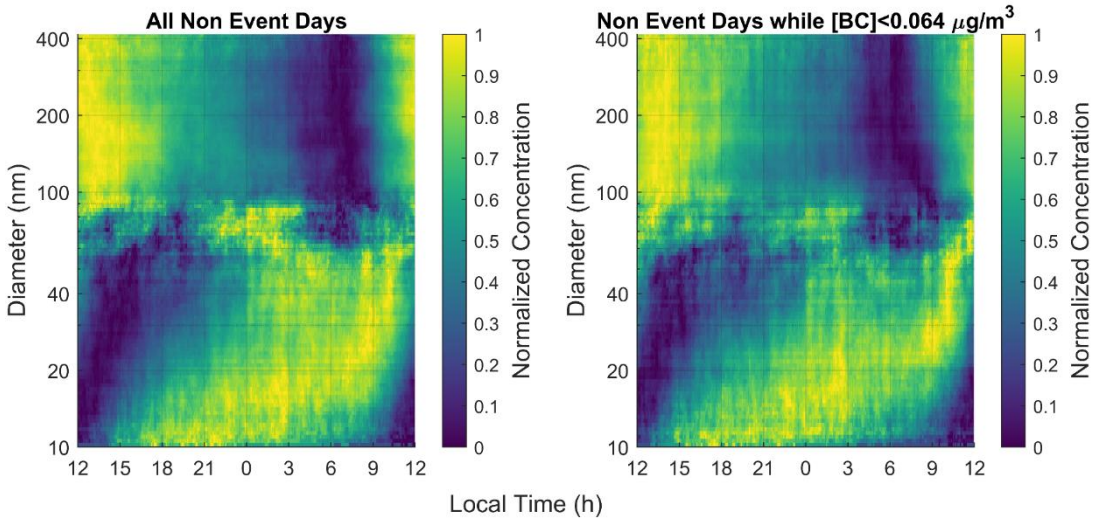


**Figure D1. Median diurnal cycle of the normalized PNSD during non-event days in the wet season at ATTO. (a) All non-event days. (b) Non-event days under low anthropogenic influence, defined by BC < 0.064 µg m⁻³.**

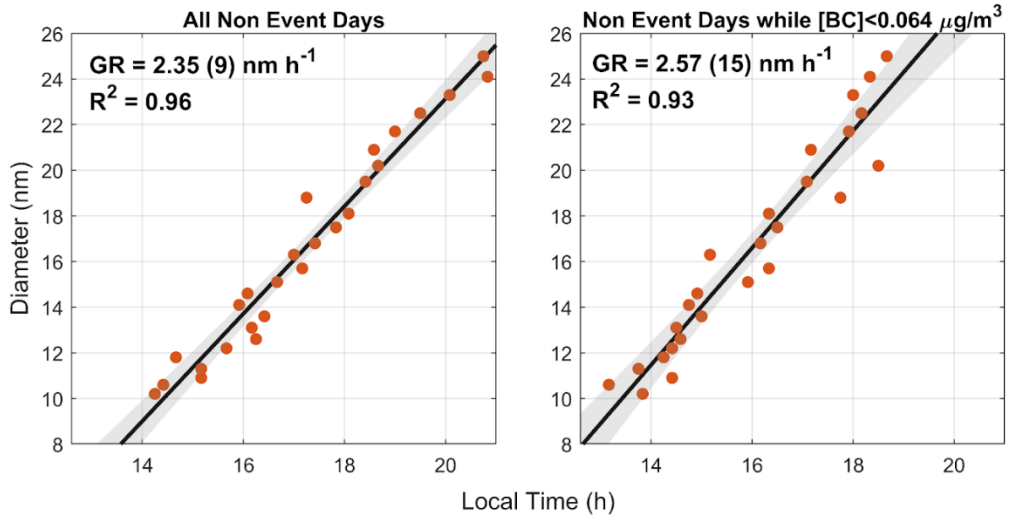


**Figure D2. Growth rate (GR) of particles between 10 and 25 nm derived using the appearance time method for non-event days during the wet season at ATTO. (a) All non-event days. (b) Non-event days under low anthropogenic influence (BC < 0.064 µg m⁻³).**

**Figure D1** shows the median diurnal cycle of the normalized PNSD for both datasets. The characteristic size-dependent temporal shift interpreted as particle formation followed by growth is consistently observed in both cases, indicating that the Quiet NPF signature is not driven by anthropogenic contamination.

**Figure D2** presents the growth rates derived for the two datasets. The GR obtained for all non-event days is 2.35 ± 0.09 nm $h^{-1}$, while the GR under low-BC conditions is 2.57 ± 0.15 nm $h^{-1}$. The two estimates are statistically consistent at the 95% confidence level.

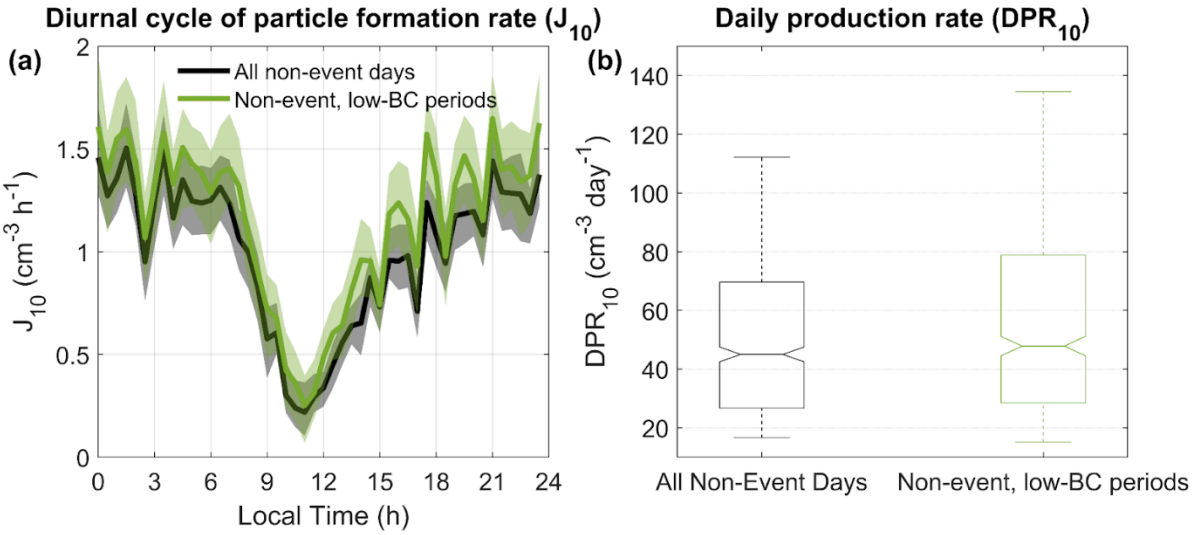


**Figure D3 - (a) Median diurnal cycle of $J_{10}$ and (b) boxplot of $DPR_{10}$ comparing all Non-event days (black) with Non-event under periods of low anthropogenic influence (green). Shaded areas on the diurnal cycle plot indicate the 95% confidence interval of the median, estimated via bootstrap.**

**Figure D3a** compares the median diurnal cycle of $J_{10}$ and the distribution of $DPR_{10}$ for the two datasets. Shaded areas indicate the 95% confidence interval of the median, estimated via bootstrap. The diurnal cycles of $J_{10}$ show overlapping confidence intervals for all time steps, indicating statistical consistency between the datasets.

**Figure D3b** shows a boxplot of the $DPR_{10}$, with medians (95% CI) of 45 (42–48) $cm^{-3}$ $day^{-1}$ for all non-event days and 48 (45–51) $cm^{-3}$ $day^{-1}$ for low-BC non-event days. A Wilcoxon rank-sum test indicates no statistically significant difference between the two $DPR_{10}$ distributions ($p > 0.01$), consistent with the overlapping uncertainty ranges of the median.

Taken together, GR, $J_{10}$, and $DPR_{10}$ do not show clear systematic differences between the two datasets. Any potential tendency toward higher values under low-BC conditions, if present, would be small and consistent with a reduced condensation sink associated with lower background particle concentrations, and does not alter the physical interpretation of the results.

These results demonstrate that the Quiet NPF identified in this study is robust and not driven by anthropogenic contamination. Retaining the full non-event-day dataset, therefore, provides a representative characterization of Quiet NPF while maximizing statistical representativeness and strengthening the robustness of the conclusions presented in the main text.

**Appendix E - Sensitivity of $J_{10}$ estimates to the formulation of the growth term**

The formation rate of 10 nm particles ($J_{10}$) is derived from the aerosol population balance equation following the framework of Kulmala et al. (2012, 2022a). In this formulation, the growth-related term can be expressed in different, but in principle equivalent, ways if particle evolution in the 10–25 nm size range is governed primarily by condensational growth and coagulation.

In the main analysis, $J_{10}$ is calculated using the product of the particle growth rate (GR) and the particle number evaluated at 25 nm $(dN/dDp)_{25}$. This choice minimizes the influence of residual inlet and counting-efficiency limitations affecting the smallest detected particles, which are particularly relevant at ATTO due to the 60 m inlet line.

For comparison and continuity with previous studies, we also evaluated $J_{10}$ using an alternative formulation in which the growth-related term is approximated by the average particle concentration between 10 and 25 nm, divided by the corresponding size interval, as used in long-term analyses (Kulmala et al., 2022a). Under ideal observational conditions, both formulations are expected to yield comparable results.

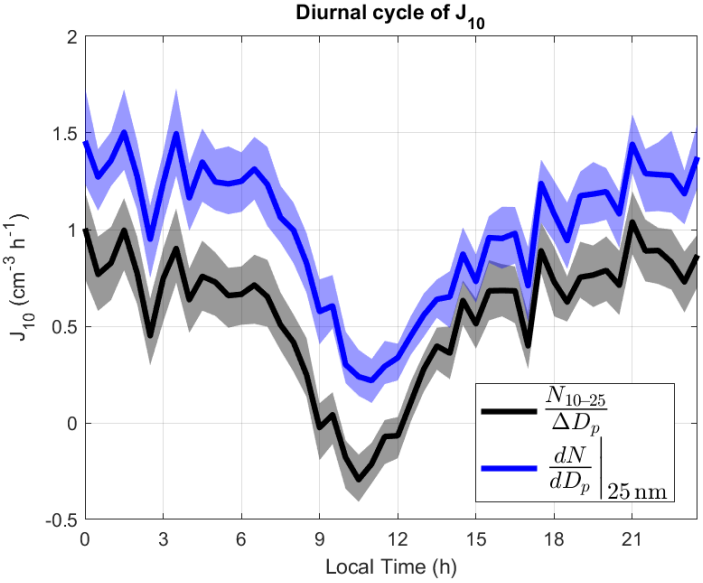


**Figure E1 - Median diurnal cycle of the particle formation rate at 10 nm ($J_{10}$) during non-event days, calculated using two formulations of the growth-related term in the aerosol population balance equation. The black curve shows $J_{10}$ derived from the average particle concentration between 10 and 25 nm, while the blue curve shows $J_{10}$ calculated using $dN/dD_p$ evaluated at 25 nm. Shaded areas on the diurnal cycle plot indicate the 95% confidence interval of the median, estimated via bootstrap.**

**Figure E1** shows the median diurnal cycle of $J_{10}$ during non-event days calculated using both formulations. The two approaches exhibit nearly identical temporal evolution throughout the day, with a high correlation ($R^2 > 0.99$, $p < 0.01$), indicating that both capture the same underlying physical process controlling sub-25 nm particle dynamics. However, the formulation based on $(dN/dD_p)_{25}$ yields systematically higher $J_{10}$ values.

This difference is attributed to size-dependent observational limitations. Particles near 25 nm experience substantially lower diffusional losses and higher counting efficiencies than particles close to the lower detection limit, whereas formulations that

rely on concentrations in the 10–25 nm range are more strongly affected by residual, sometimes uncorrectable, losses when individual bins approach zero counts. These effects result in low bias in $J_{10}$ estimates derived from the integrated 10–25 nm formulation under ATTO measurement conditions.

Importantly, the higher $J_{10}$ values obtained using $(dN/dD_p)_{25}$ represent a proportional shift affecting both event and non-event days, and therefore do not alter the inferred relative contribution of Quiet New Particle Formation to total 10–25 nm particle production. Instead, they provide a more robust quantitative estimate of absolute formation and production rates under conditions where losses at the smallest sizes cannot be fully corrected due to zero-count limitations.

For these reasons, the main text adopts the $(dN/dD_p)_{25}$ formulation for $J_{10}$, whereas this appendix presents a sensitivity analysis to ensure transparency and comparability with earlier methodological approaches.

## Appendix F - Percentile-based analysis of Quiet NPF occurrence on non-event days

Quiet New Particle Formation (Quiet NPF) is characterized by very low particle concentrations and, in the Amazon, slow growth rates, which generally preclude its identification at the scale of individual daily PNSDs. This limitation is particularly relevant at ATTO, where measurements at 60 m height are affected by inlet line losses, air-mass heterogeneity, and low signal-to-noise ratios in the sub-25 nm size range. As discussed by Kulmala et al. (2022a), normalization and ensemble averaging are essential for revealing the statistical signature of this process.

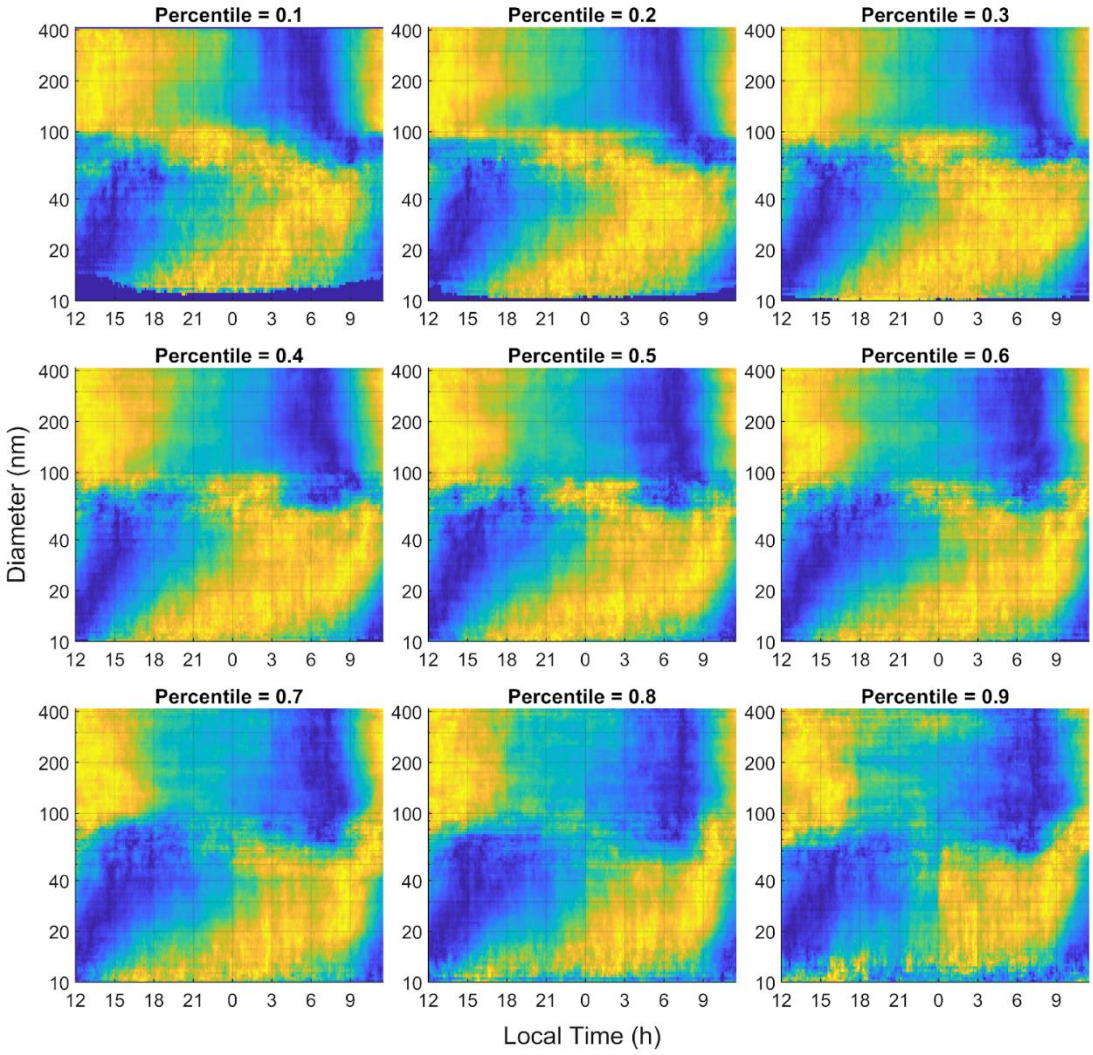


**Figure F1. Diurnal evolution of the normalized particle number size distribution during non-event days is shown for different concentration percentiles (10th to 90th, in steps of 10%). The characteristic slow and sequential increase in particle diameter is consistently observed across a wide range of percentiles, demonstrating that the Quiet NPF signature is a general statistical property of non-event days and not an artefact of averaging or of a small subset of high-concentration days.**

To explicitly test whether the Quiet NPF signature identified in this study (characterized in the main text using the median normalized PNSD) reflects a general property of non-event days rather than an artefact of averaging or a limited subset of days, we extended the analysis by examining different percentiles of the normalized PNSD. **Figure F1** shows the diurnal evolution of particle size distributions for percentiles ranging from the 10th to the 90th percentile, calculated independently for each size bin and local time.

Across a broad range of percentiles, particularly from the 10th to the 80th percentiles, the normalized PNSDs exhibit a gradual and sequential increase in particle diameter over time, consistent with particle formation followed by growth. The

persistence of this pattern across percentiles demonstrates that the Quiet NPF signature is not dominated by high-concentration outliers or by a small number of specific days, but instead reflects a systematic statistical feature of non-event days in the Amazon boundary layer.

While this result supports the interpretation that Quiet NPF is a phenomenon virtually always present on non-event days across a wide range of intensities, it does not imply that the process is spatially homogeneous, i.e., that it has a continuous intensity over large regions. The formation and growth of new particles depend on atmospheric conditions that vary in space and time, such as oxidation capacity, precursor availability, meteorology, and air-mass history. The observed ensemble behaviour is therefore consistent with a scenario in which particle formation occurs heterogeneously in space and time, potentially within localized air masses, and becomes detectable only through statistical aggregation across many realizations. Together with the normalized median analysis presented in the main text, the percentile-based results confirm that ensemble averaging does not artificially generate the observed growth pattern but instead reveals the underlying statistical imprint of a weak yet pervasive particle-formation process in the Amazon boundary layer.

## Data availability

Data will be openly available at Edmond, the Open Research Data Repository of the Max Planck Society, at the time of publication. Currently, data is temporarily available at http://ftp.lfa.if.usp.br/ftp/public/Temp/Edmond_Meller2025_Paper/.

## Author Contribution

B. B. Meller conceived the study, processed data, performed the analyses, and prepared the manuscript. M. A. Franco and R. Valiati processed data and contributed to the analysis and interpretation. C. Pöhlker, F. Ditas, L. A. Kremper, S. S. Raj, C. Q. Dias-Júnior, and F. A. F. D'Oliveira carried out field measurements at ATTO and processed. L. V. Rizzo, C. Pöhlker, L. A. T. Machado, U. Pöschl, and P. Artaxo contributed to supervision, project administration, and funding acquisition. All authors contributed to the discussion of results and to reviewing and editing the manuscript.

## Competing Interests

Some authors are members of the editorial board of the journal Atmospheric Chemistry and Physics.

## Acknowledgements

We are deeply grateful to all colleagues who have provided technical, logistical, and scientific support for the ATTO project.

**Financial support**

B. B. Meller thanks FAPESP for grants Nº 2020/15405-0 and 2023/01902-0. P. Artaxo thanks FAPESP for the grant 2023/04358-9. L.A.T. Machado thanks FAPESP for the grant Nº 2022/07974-0. We gratefully acknowledge the German Federal Ministry of Education and Research (BMBF, contracts 01LB1001A and 01LK2101B) and the Max Planck Society for their support of this project and the construction and operation of the ATTO site. We also extend our gratitude to the Brazilian Ministério da Ciência, Tecnologia e Inovação (MCTI/FINEP), as well as the Amazon State University (UEA), FAPEAM, LBA/INPA, and SDS/CEUC/RDS-Uatumã for their contributions to the construction and operation of the ATTO site.

**References**

Aliaga, D., Tuovinen, S., Zhang, T., Lampilahti, J., Li, X., Ahonen, L., Kokkonen, T., Nieminen, T., Hakala, S., Paasonen, P., Bianchi, F., Worsnop, D., Kerminen, V.-M., and Kulmala, M.: Nanoparticle ranking analysis: determining new particle formation (NPF) event occurrence and intensity based on the concentration spectrum of formed (sub-50 nm) particles, Aerosol Research, 1, 81–92, https://doi.org/10.5194/ar-1-81-2023, 2023.

Andreae, M. O., Acevedo, O. C., Araùjo, A., Artaxo, P., Barbosa, C. G. G., Barbosa, H. M. J., Brito, J., Carbone, S., Chi, X., Cintra, B. B. L., da Silva, N. F., Dias, N. L., Dias-Júnior, C. Q., Ditas, F., Ditz, R., Godoi, A. F. L., Godoi, R. H. M., Heimann, M., Hoffmann, T., Kesselmeier, J., Könemann, T., Krüger, M. L., Lavric, J. V., Manzi, A. O., Lopes, A. P., Martins, D. L., Mikhailov, E. F., Moran-Zuloaga, D., Nelson, B. W., Nölscher, A. C., Santos Nogueira, D., Piedade, M. T. F., Pöhlker, C., Pöschl, U., Quesada, C. A., Rizzo, L. V., Ro, C.-U., Ruckteschler, N., Sá, L. D. A., de Oliveira Sá, M., Sales, C. B., dos Santos, R. M. N., Saturno, J., Schöngart, J., Sörgel, M., de Souza, C. M., de Souza, R. a. F., Su, H., Targhetta, N., Tóta, J., Trebs, I., Trumbore, S., van Eijck, A., Walter, D., Wang, Z., Weber, B., Williams, J., Winderlich, J., Wittmann, F., Wolff, S., and Yáñez-Serrano, A. M.: The Amazon Tall Tower Observatory (ATTO): overview of pilot measurements on ecosystem ecology, meteorology, trace gases, and aerosols, Atmospheric Chemistry and Physics, 15, 10723–10776, https://doi.org/10.5194/acp-15-10723-2015, 2015.

Andreae, M. O., Afchine, A., Albrecht, R., Holanda, B. A., Artaxo, P., Barbosa, H. M. J., Borrmann, S., Cecchini, M. A., Costa, A., Dollner, M., Fütterer, D., Järvinen, E., Jurkat, T., Klimach, T., Konemann, T., Knote, C., Krämer, M., Krisna, T., Machado, L. A. T., Mertes, S., Minikin, A., Pöhlker, C., Pöhlker, M. L., Pöschl, U., Rosenfeld, D., Sauer, D., Schlager, H., Schnaiter, M., Schneider, J., Schulz, C., Spanu, A., Sperling, V. B., Voigt, C., Walser, A., Wang, J., Weinzierl, B., Wendisch, M., and Ziereis, H.: Aerosol characteristics and particle production in the upper troposphere over the Amazon Basin, Atmos. Chem. Phys., 18, 921–961, https://doi.org/10.5194/acp-18-921-2018, 2018.

Artaxo, P., Rizzo, L. V., Brito, J. F., Barbosa, H. M. J., Arana, A., Sena, E. T., Cirino, G. G., Bastos, W., Martin, S. T., and Andreae, M. O.: Atmospheric aerosols in Amazonia and land use change: from natural biogenic to biomass burning conditions, Faraday Discuss., 165, 203–235, https://doi.org/10.1039/C3FD00052D, 2013.

Artaxo, P., Hansson, H.-C., Andreae, M. O., Bäck, J., Alves, E. G., Barbosa, H. M. J., Bender, F., Bourtsoukidis, E., Carbone, S., Chi, J., Decesari, S., Després, V. R., Ditas, F., Ezhova, E., Fuzzi, S., Hasselquist, N. J., Heintzenberg, J., Holanda, B. A., Guenther, A., Hakola, H., Heikkinen, L., Kerminen, V.-M., Kontkanen, J., Krejci, R., Kulmala, M., Lavric, J. V., De Leeuw, G., Lehtipalo, K., Machado, L. A. T., McFiggans, G., Franco, M. A. M., Meller, B. B., Morais, F. G., Mohr, C., Morgan, W., Nilsson, M. B., Peichl, M., Petäjä, T., Praß, M., Pöhlker, C., Pöhlker, M. L., Pöschl, U., Von Randow, C., Riipinen, I., Rinne, J., Rizzo, L. V., Rosenfeld, D., Silva Dias, M. A. F., Sogacheva, L., Stier, P., Swietlicki, E., Sörgel, M., Tunved, P., Virkkula, A., Wang, J., Weber, B., Yáñez-Serrano, A. M., Zieger, P., Mikhailov, E., Smith, J. N., and Kesselmeier, J.: Tropical and Boreal Forest – Atmosphere Interactions: A Review, Tellus B: Chemical and Physical Meteorology, 74, 24, https://doi.org/10.16993/tellusb.34, 2022.

Bardakov, R., Thornton, J. A., Ekman, A. M. L., Krejci, R., Pöhlker, M. L., Curtius, J., Williams, J., Lelieveld, J., and Riipinen, I.: High Concentrations of Nanoparticles From Isoprene Nitrates Predicted in Convective Outflow Over the Amazon, Geophysical Research Letters, 51, e2024GL109919, https://doi.org/10.1029/2024GL109919, 2024.

Chen, L., Qi, X., Niu, G., Li, Y., Liu, C., Lai, S., Liu, Y., Nie, W., Yan, C., Wang, J., Chi, X., Paasonen, P., Hussein, T., Lehtipalo, K., Kerminen, V.-M., Petäjä, T., Kulmala, M., and Ding, A.: High Concentration of Atmospheric Sub-3 nm Particles in Polluted Environment of Eastern China: New Particle Formation and Traffic Emission, Journal of Geophysical Research: Atmospheres, 128, e2023JD039669, https://doi.org/10.1029/2023JD039669, 2023.

Chen, Q., Farmer, D. K., Rizzo, L. V., Pauliquevis, T., Kuwata, M., Karl, T. G., Guenther, A., Allan, J. D., Coe, H., Andreae, M. O., Pöschl, U., Jimenez, J. L., Artaxo, P., and Martin, S. T.: Submicron particle mass concentrations and sources in the Amazonian wet season (AMAZE-08), Atmospheric Chemistry and Physics, 15, 3687–3701, https://doi.org/10.5194/acp-15-3687-2015, 2015.

Curtius, J., Heinritzi, M., Beck, L. J., Pöhlker, M. L., Tripathi, N., Krumm, B. E., Holzbeck, P., Nussbaumer, C. M., Hernández Pardo, L., Klimach, T., Barmpounis, K., Andersen, S. T., Bardakov, R., Bohn, B., Cecchini, M. A., Chaboureau, J.-P., Dauhut, T., Dienhart, D., Dörich, R., Edtbauer, A., Giez, A., Hartmann, A., Holanda, B. A., Joppe, P., Kaiser, K., Keber, T., Klebach, H., Krüger, O. O., Kürten, A., Mallaun, C., Marno, D., Martinez, M., Monteiro, C., Nelson, C., Ort, L., Raj, S. S., Richter, S., Ringsdorf, A., Rocha, F., Simon, M., Sreekumar, S., Tsokankunku, A., Unfer, G. R., Valenti, I. D., Wang, N., Zahn, A., Zauner-Wieczorek, M., Albrecht, R. I., Andreae, M. O., Artaxo, P., Crowley, J. N., Fischer, H., Harder, H., Herdies, D. L., Machado, L. A. T., Pöhlker, C., Pöschl, U., Possner, A., Pozzer, A., Schneider, J., Williams, J., and Lelieveld, J.: Isoprene nitrates drive new particle formation in Amazon's upper troposphere, Nature, 636, 124–130, https://doi.org/10.1038/s41586-024-08192-4, 2024.

Dal Maso, M., Kulmala, M., Riipinen, I., Wagner, R., Hussein, T., Aalto, P. P., and Lehtinen, K. E. J.: Formation and growth of fresh atmospheric aerosols: eight years of aerosol size distribution data from SMEAR II, Hyytiälä, Finland, Boreal Environment Research, 10, 323–336, 2005.

Dada, L., Chellapermal, R., Buenrostro Mazon, S., Paasonen, P., Lampilahti, J., Manninen, H. E., Junninen, H., Petäjä, T., Kerminen, V.-M., and Kulmala, M.: Refined classification and characterization of atmospheric new-particle formation

events using air ions, Atmospheric Chemistry and Physics, 18, 17883–17893, https://doi.org/10.5194/acp-18-17883-2018, 2018.

Dada, L., Stolzenburg, D., Simon, M., Fischer, L., Heinritzi, M., Wang, M., Xiao, M., Vogel, A. L., Ahonen, L., Amorim, A., Baalbaki, R., Baccarini, A., Baltensperger, U., Bianchi, F., Daellenbach, K. R., DeVivo, J., Dias, A., Dommen, J., Duplissy, J., Finkenzeller, H., Hansel, A., He, X.-C., Hofbauer, V., Hoyle, C. R., Kangasluoma, J., Kim, C., Kürten, A., Kvashnin, A., Mauldin, R., Makhmutov, V., Marten, R., Mentler, B., Nie, W., Petäjä, T., Quéléver, L. L. J., Saathoff, H., Tauber, C., Tome, A., Molteni, U., Volkamer, R., Wagner, R., Wagner, A. C., Wimmer, D., Winkler, P. M., Yan, C., Zha, Q., Rissanen, M., Gordon, H., Curtius, J., Worsnop, D. R., Lehtipalo, K., Donahue, N. M., Kirkby, J., El Haddad, I., and Kulmala, M.: Role of sesquiterpenes in biogenic new particle formation, Sci. Adv., 9, eadi5297, https://doi.org/10.1126/sciadv.adi5297, 2023.

Dias-Junior, C. Q., Dias, N. L., Fuentes, J. D., and Chamecki, M.: Convective storms and non-classical low-level jets during high ozone level episodes in the Amazon region: An ARM/GOAMAZON case study, Atmospheric Environment, 155, 199–209, https://doi.org/10.1016/j.atmosenv.2017.02.006, 2017.

Franco, M. A., Ditas, F., Kremper, L. A., Machado, L. A. T., Andreae, M. O., Araújo, A., Barbosa, H. M. J., de Brito, J. F., Carbone, S., Holanda, B. A., Morais, F. G., Nascimento, J. P., Pöhlker, M. L., Rizzo, L. V., Sá, M., Saturno, J., Walter, D., Wolff, S., Pöschl, U., Artaxo, P., and Pöhlker, C.: Occurrence and growth of sub-50 nm aerosol particles in the Amazonian boundary layer, Atmospheric Chemistry and Physics, 22, 3469–3492, https://doi.org/10.5194/acp-22-3469-2022, 2022.

Franco, M. A., Valiati, R., Holanda, B. A., Meller, B. B., Kremper, L. A., Rizzo, L. V., Carbone, S., Morais, F. G., Nascimento, J. P., Andreae, M. O., Cecchini, M. A., Machado, L. A. T., Ponczek, M., Pöschl, U., Walter, D., Pöhlker, C., and Artaxo, P.: Vertically resolved aerosol variability at the Amazon Tall Tower Observatory under wet-season conditions, Atmospheric Chemistry and Physics, 24, 8751–8770, https://doi.org/10.5194/acp-24-8751-2024, 2024.

Gerken, T., Wei, D., Chase, R. J., Fuentes, J. D., Schumacher, C., Machado, L. A. T., Andreoli, R. V., Chamecki, M., Ferreira De Souza, R. A., Freire, L. S., Jardine, A. B., Manzi, A. O., Nascimento Dos Santos, R. M., Von Randow, C., Dos Santos Costa, P., Stoy, P. C., Tóta, J., and Trowbridge, A. M.: Downward transport of ozone rich air and implications for atmospheric chemistry in the Amazon rainforest, Atmospheric Environment, 124, 64–76, https://doi.org/10.1016/j.atmosenv.2015.11.014, 2016.

Glicker, H. S., Lawler, M. J., Ortega, J., de Sá, S. S., Martin, S. T., Artaxo, P., Vega Bustillos, O., de Souza, R., Tota, J., Carlton, A., and Smith, J. N.: Chemical composition of ultrafine aerosol particles in central Amazonia during the wet season, Atmospheric Chemistry and Physics, 19, 13053–13066, https://doi.org/10.5194/acp-19-13053-2019, 2019.

Gordon, H., Kirkby, J., Baltensperger, U., Bianchi, F., Breitenlechner, M., Curtius, J., Dias, A., Dommen, J., Donahue, N. M., Dunne, E. M., Duplissy, J., Ehrhart, S., Flagan, R. C., Frege, C., Fuchs, C., Hansel, A., Hoyle, C. R., Kulmala, M., Kürten, A., Lehtipalo, K., Makhmutov, V., Molteni, U., Rissanen, M. P., Stozkhov, Y., Tröstl, J., Tsagkogeorgas, G., Wagner, R., Williamson, C., Wimmer, D., Winkler, P. M., Yan, C., and Carslaw, K. S.: Causes and importance of new

particle formation in the present-day and preindustrial atmospheres, Journal of Geophysical Research: Atmospheres, 122, 8739–8760, https://doi.org/10.1002/2017JD026844, 2017.

Heinritzi, M., Dada, L., Simon, M., Stolzenburg, D., Wagner, A. C., Fischer, L., Ahonen, L. R., Amanatidis, S., Baalbaki, R., Baccarini, A., Bauer, P. S., Baumgartner, B., Bianchi, F., Brilke, S., Chen, D., Chiu, R., Dias, A., Dommen, J., Duplissy, J., Finkenzeller, H., Frege, C., Fuchs, C., Garmash, O., Gordon, H., Granzin, M., El Haddad, I., He, X., Helm, J., Hofbauer, V., Hoyle, C. R., Kangasluoma, J., Keber, T., Kim, C., Kürten, A., Lamkaddam, H., Laurila, T. M., Lampilahti, J., Lee, C. P., Lehtipalo, K., Leiminger, M., Mai, H., Makhmutov, V., Manninen, H. E., Marten, R., Mathot, S., Mauldin, R. L., Mentler, B., Molteni, U., Müller, T., Nie, W., Nieminen, T., Onnela, A., Partoll, E., Passananti, M., Petäjä, T., Pfeifer, J., Pospisilova, V., Quéléver, L. L. J., Rissanen, M. P., Rose, C., Schobesberger, S., Scholz, W., Scholze, K., Sipilä, M., Steiner, G., Stozhkov, Y., Tauber, C., Tham, Y. J., Vazquez-Pufleau, M., Virtanen, A., Vogel, A. L., Volkamer, R., Wagner, R., Wang, M., Weitz, L., Wimmer, D., Xiao, M., Yan, C., Ye, P., Zha, Q., Zhou, X., Amorim, A., Baltensperger, U., Hansel, A., Kulmala, M., Tomé, A., Winkler, P. M., Worsnop, D. R., Donahue, N. M., Kirkby, J., and Curtius, J.: Molecular understanding of the suppression of new-particle formation by isoprene, Atmospheric Chemistry and Physics, 20, 11809–11821, https://doi.org/10.5194/acp-20-11809-2020, 2020.

Holanda, B. A., Franco, M. A., Walter, D., Artaxo, P., Carbone, S., Cheng, Y., Chowdhury, S., Ditas, F., Gysel-Beer, M., Klimach, T., Kremper, L. A., Krüger, O. O., Lavric, J. V., Lelieveld, J., Ma, C., Machado, L. A. T., Modini, R. L., Morais, F. G., Pozzer, A., Saturno, J., Su, H., Wendisch, M., Wolff, S., Pöhlker, M. L., Andreae, M. O., Pöschl, U., and Pöhlker, C.: African biomass burning affects aerosol cycling over the Amazon, Commun Earth Environ, 4, 154, https://doi.org/10.1038/s43247-023-00795-5, 2023.

Kerminen, V.-M., Pirjola, L., and Kulmala, M.: How significantly does coagulational scavenging limit atmospheric particle production?, Journal of Geophysical Research: Atmospheres, 106, 24119–24125, https://doi.org/10.1029/2001JD000322, 2001.

Kerminen, V.-M., Chen, X., Vakkari, V., Petäjä, T., Kulmala, M., and Bianchi, F.: Atmospheric new particle formation and growth: review of field observations, Environ. Res. Lett., 13, 103003, https://doi.org/10.1088/1748-9326/aadf3c, 2018.

Kirkby, J., Amorim, A., Baltensperger, U., Carslaw, K. S., Christoudias, T., Curtius, J., Donahue, N. M., Haddad, I. E., Flagan, R. C., Gordon, H., Hansel, A., Harder, H., Junninen, H., Kulmala, M., Kürten, A., Laaksonen, A., Lehtipalo, K., Lelieveld, J., Möhler, O., Riipinen, I., Stratmann, F., Tomé, A., Virtanen, A., Volkamer, R., Winkler, P. M., and Worsnop, D. R.: Atmospheric new particle formation from the CERN CLOUD experiment, Nat. Geosci., 16, 948–957, https://doi.org/10.1038/s41561-023-01305-0, 2023.

Kulmala, M., Petäjä, T., Nieminen, T., Sipilä, M., Manninen, H. E., Lehtipalo, K., Dal Maso, M., Aalto, P. P., Junninen, H., Paasonen, P., Riipinen, I., Lehtinen, K. E. J., Laaksonen, A., and Kerminen, V.-M.: Measurement of the nucleation of atmospheric aerosol particles, Nat Protoc, 7, 1651–1667, https://doi.org/10.1038/nprot.2012.091, 2012.

Kulmala, M., Kontkanen, J., Junninen, H., Lehtipalo, K., Manninen, H. E., Nieminen, T., Petäjä, T., Sipilä, M., Schobesberger, S., Rantala, P., Franchin, A., Jokinen, T., Järvinen, E., Äijälä, M., Kangasluoma, J., Hakala, J., Aalto, P. P.,

Paasonen, P., Mikkilä, J., Vanhanen, J., Aalto, J., Hakola, H., Makkonen, U., Ruuskanen, T., Mauldin, R. L., Duplissy, J., Vehkamäki, H., Bäck, J., Kortelainen, A., Riipinen, I., Kurtén, T., Johnston, M. V., Smith, J. N., Ehn, M., Mentel, T. F., Lehtinen, K. E. J., Laaksonen, A., Kerminen, V.-M., and Worsnop, D. R.: Direct Observations of Atmospheric Aerosol Nucleation, Science, 339, 943–946, https://doi.org/10.1126/science.1227385, 2013.

Kulmala, M., Junninen, H., Dada, L., Salma, I., Weidinger, T., Thén, W., Vörösmarty, M., Komsaare, K., Stolzenburg, D., Cai, R., Yan, C., Li, X., Deng, C., Jiang, J., Petäjä, T., Nieminen, T., and Kerminen, V.-M.: Quiet New Particle Formation in the Atmosphere, Front. Environ. Sci., 10, 912385, https://doi.org/10.3389/fenvs.2022.912385, 2022a.

Kulmala, M., Cai, R., Stolzenburg, D., Zhou, Y., Dada, L., Guo, Y., Yan, C., Petäjä, T., Jiang, J., and Kerminen, V.-M.: The contribution of new particle formation and subsequent growth to haze formation, Environ. Sci.: Atmos., 2, 352–361, https://doi.org/10.1039/D1EA00096A, 2022b.

Kulmala, M., Aliaga, D., Tuovinen, S., Cai, R., Junninen, H., Yan, C., Bianchi, F., Cheng, Y., Ding, A., Worsnop, D. R., Petäjä, T., Lehtipalo, K., Paasonen, P., and Kerminen, V.-M.: Opinion: A paradigm shift in investigating the general characteristics of atmospheric new particle formation using field observations, Aerosol Research, 2, 49–58, https://doi.org/10.5194/ar-2-49-2024, 2024.

Lehtipalo, K., Leppä, J., Kontkanen, J., Kangasluoma, J., Franchin, A., Wimnner, D., Schobesberger, S., Junninen, H., Petäjä, T., Sipilä, M., Mikkilä, J., Vanhanen, J., Worsnop, D. R., and Kulmala, M.: Methods for determining particle size distribution and growthrates between 1 and 3 nm using the Particle Size Magnifier, Boreal Environment Research, 19(B), 215–236, 2014.

Liu, Y., Su, H., Wang, S., Wei, C., Tao, W., Pöhlker, M. L., Pöhlker, C., Holanda, B. A., Krüger, O. O., Hoffmann, T., Wendisch, M., Artaxo, P., Pöschl, U., Andreae, M. O., and Cheng, Y.: Strong particle production and condensational growth in the upper troposphere sustained by biogenic VOCs from the canopy of the Amazon Basin, Atmospheric Chemistry and Physics, 23, 251–272, https://doi.org/10.5194/acp-23-251-2023, 2023.

Machado, L. A. T., Franco, M. A., Kremper, L. A., Ditas, F., Andreae, M. O., Artaxo, P., Cecchini, M. A., Holanda, B. A., Pöhlker, M. L., Saraiva, I., Wolff, S., Pöschl, U., and Pöhlker, C.: How weather events modify aerosol particle size distributions in the Amazon boundary layer, Atmospheric Chemistry and Physics, 21, 18065–18086, https://doi.org/10.5194/acp-21-18065-2021, 2021.

Machado, L. A. T., Unfer, G. R., Brill, S., Hildmann, S., Pöhlker, C., Cheng, Y., Williams, J., Hartwig, H., Andreae, M. O., Artaxo, P., Curtius, J., Franco, M. A., Cecchini, M. A., Edtbauer, A., Hoffmann, T., Holanda, B., Khadir, T., Krejci, R., Kremper, L. A., Liu, Y., Meller, B. B., Pöhlker, M. L., Quesada, C. A., Ringsdorf, A., Riipinen, I., Trumbore, S., Wolff, S., Lelieveld, J., and Pöschl, U.: Frequent rainfall-induced new particle formation within the canopy in the Amazon rainforest, Nat. Geosci., 17, 1225–1232, https://doi.org/10.1038/s41561-024-01585-0, 2024.

Mohr, C., Thornton, J. A., Heitto, A., Lopez-Hilfiker, F. D., Lutz, A., Riipinen, I., Hong, J., Donahue, N. M., Hallquist, M., Petäjä, T., Kulmala, M., and Yli-Juuti, T.: Molecular identification of organic vapors driving atmospheric nanoparticle growth, Nat Commun, 10, 4442, https://doi.org/10.1038/s41467-019-12473-2, 2019.

Pöhlker, C., Wiedemann, K. T., Sinha, B., Shiraiwa, M., Gunthe, S. S., Smith, M., Su, H., Artaxo, P., Chen, Q., Cheng, Y., Elbert, W., Gilles, M. K., Kilcoyne, A. L. D., Moffet, R. C., Weigand, M., Martin, S. T., Pöschl, U., and Andreae, M. O.: Biogenic Potassium Salt Particles as Seeds for Secondary Organic Aerosol in the Amazon, Science, 337, 1075–1078, https://doi.org/10.1126/science.1223264, 2012.

Pöhlker, M. L., Pöhlker, C., Ditas, F., Klimach, T., Hrabe de Angelis, I., Araújo, A., Brito, J., Carbone, S., Cheng, Y., Chi, X., Ditz, R., Gunthe, S. S., Kesselmeier, J., Könemann, T., Lavrič, J. V., Martin, S. T., Mikhailov, E., Moran-Zuloaga, D., Rose, D., Saturno, J., Su, H., Thalman, R., Walter, D., Wang, J., Wolff, S., Barbosa, H. M. J., Artaxo, P., Andreae, M. O., and Pöschl, U.: Long-term observations of cloud condensation nuclei in the Amazon rain forest – Part 1: Aerosol size distribution, hygroscopicity, and new model parametrizations for CCN prediction, Atmospheric Chemistry and Physics, 16, 15709–15740, https://doi.org/10.5194/acp-16-15709-2016, 2016.

Pöhlker, M. L., Ditas, F., Saturno, J., Klimach, T., Hrabě de Angelis, I., Araújo, A. C., Brito, J., Carbone, S., Cheng, Y., Chi, X., Ditz, R., Gunthe, S. S., Holanda, B. A., Kandler, K., Kesselmeier, J., Könemann, T., Krüger, O. O., Lavrič, J. V., Martin, S. T., Mikhailov, E., Moran-Zuloaga, D., Rizzo, L. V., Rose, D., Su, H., Thalman, R., Walter, D., Wang, J., Wolff, S., Barbosa, H. M. J., Artaxo, P., Andreae, M. O., Pöschl, U., and Pöhlker, C.: Long-term observations of cloud condensation nuclei over the Amazon rain forest – Part 2: Variability and characteristics of biomass burning, long-range transport, and pristine rain forest aerosols, Atmos. Chem. Phys., 18, 10289–10331, https://doi.org/10.5194/acp-18-10289-2018, 2018.

Pöschl, U., Martin, S. T., Sinha, B., Chen, Q., Gunthe, S. S., Huffman, J. A., Borrmann, S., Farmer, D. K., Garland, R. M., Helas, G., Jimenez, J. L., King, S. M., Manzi, A., Mikhailov, E., Pauliquevis, T., Petters, M. D., Prenni, A. J., Roldin, P., Rose, D., Schneider, J., Su, H., Zorn, S. R., Artaxo, P., and Andreae, M. O.: Rainforest Aerosols as Biogenic Nuclei of Clouds and Precipitation in the Amazon, Science, 329, 1513–1516, https://doi.org/10.1126/science.1191056, 2010.

Rizzo, L. V., Roldin, P., Brito, J., Backman, J., Swietlicki, E., Krejci, R., Tunved, P., Petäjä, T., Kulmala, M., and Artaxo, P.: Multi-year statistical and modeling analysis of submicrometer aerosol number size distributions at a rain forest site in Amazonia, Atmospheric Chemistry and Physics, 18, 10255–10274, https://doi.org/10.5194/acp-18-10255-2018, 2018.

Saturno, J., Holanda, B. A., Pöhlker, C., Ditas, F., Wang, Q., Moran-Zuloaga, D., Brito, J., Carbone, S., Cheng, Y., Chi, X., Ditas, J., Hoffmann, T., Hrabe de Angelis, I., Könemann, T., Lavrič, J. V., Ma, N., Ming, J., Paulsen, H., Pöhlker, M. L., Rizzo, L. V., Schlag, P., Su, H., Walter, D., Wolff, S., Zhang, Y., Artaxo, P., Pöschl, U., and Andreae, M. O.: Black and brown carbon over central Amazonia: long-term aerosol measurements at the ATTO site, Atmospheric Chemistry and Physics, 18, 12817–12843, https://doi.org/10.5194/acp-18-12817-2018, 2018.

Schervish, M. and Donahue, N. M.: Peroxy radical chemistry and the volatility basis set, Atmospheric Chemistry and Physics, 20, 1183–1199, https://doi.org/10.5194/acp-20-1183-2020, 2020.

Seinfeld, J. H. and Pandis, S. N.: Atmospheric Chemistry and Physics: From Air Pollution to Climate Change, John Wiley & Sons, 1249 pp., 2012.

Shen, J., Russell, D. M., DeVivo, J., Kunkler, F., Baalbaki, R., Mentler, B., Scholz, W., Yu, W., Caudillo-Plath, L., Sommer, E., Ahongshangbam, E., Alfaouri, D., Almeida, J., Amorim, A., Beck, L. J., Beckmann, H., Berntheusel, M., Bhattacharyya,

N., Canagaratna, M. R., Chassaing, A., Cruz-Simbron, R., Dada, L., Duplissy, J., Gordon, H., Granzin, M., Große Schute, L., Heinritzi, M., Iyer, S., Klebach, H., Krüger, T., Kürten, A., Lampimäki, M., Liu, L., Lopez, B., Martinez, M., Morawiec, A., Onnela, A., Peltola, M., Rato, P., Reza, M., Richter, S., Rörup, B., Sebastian, M. K., Simon, M., Surdu, M., Tamme, K., Thakur, R. C., Tomé, A., Tong, Y., Top, J., Umo, N. S., Unfer, G., Vettikkat, L., Weissbacher, J., Xenofontos, C., Yang, B., Zauner-Wieczorek, M., Zhang, J., Zheng, Z., Baltensperger, U., Christoudias, T., Flagan, R. C., El Haddad, I., Junninen, H., Möhler, O., Riipinen, I., Rohner, U., Schobesberger, S., Volkamer, R., Winkler, P. M., Hansel, A., Lehtipalo, K., Donahue, N. M., Lelieveld, J., Harder, H., Kulmala, M., Worsnop, D. R., Kirkby, J., Curtius, J., and He, X.-C.: New particle formation from isoprene under upper-tropospheric conditions, Nature, 636, 115–123, https://doi.org/10.1038/s41586-024-08196-0, 2024.

Spracklen, D. V., Arnold, S. R., Sciare, J., Carslaw, K. S., and Pio, C.: Globally significant oceanic source of organic carbon aerosol, Geophysical Research Letters, 35, https://doi.org/10.1029/2008GL033359, 2008.

Valiati, R., Meller, B. B., Franco, M. A., Rizzo, L. V., Machado, L. A., Brill, S., and Artaxo, P.: Distinct aerosol populations and their vertical gradients in central Amazonia revealed by optical properties and cluster analysis, *Atmos. Chem. Phys.*, **25**, 14923–14944, https://doi.org/10.5194/acp-25-14923-2025, 2025.

Wang, J., Krejci, R., Giangrande, S., Kuang, C., Barbosa, H. M. J., Brito, J., Carbone, S., Chi, X., Comstock, J., Ditas, F., Lavric, J., Manninen, H. E., Mei, F., Moran-Zuloaga, D., Pöhlker, C., Pöhlker, M. L., Saturno, J., Schmid, B., Souza, R. A. F., Springston, S. R., Tomlinson, J. M., Toto, T., Walter, D., Wimmer, D., Smith, J. N., Kulmala, M., Machado, L. A. T., Artaxo, P., Andreae, M. O., Petäjä, T., and Martin, S. T.: Amazon boundary layer aerosol concentration sustained by vertical transport during rainfall, Nature, 539, 416–419, https://doi.org/10.1038/nature19819, 2016.

Wang, X., Gordon, H., Grosvenor, D. P., Andreae, M. O., and Carslaw, K. S.: Contribution of regional aerosol nucleation to low-level CCN in an Amazonian deep convective environment: results from a regionally nested global model, Atmospheric Chemistry and Physics, 23, 4431–4461, https://doi.org/10.5194/acp-23-4431-2023, 2023.

von der Weiden, S.-L., Drewnick, F., and Borrmann, S.: Particle Loss Calculator – a new software tool for the assessment of the performance of aerosol inlet systems, Atmospheric Measurement Techniques, 2, 479–494, https://doi.org/10.5194/amt-2-479-2009, 2009.

Yáñez-Serrano, A. M., Nölscher, A. C., Williams, J., Wolff, S., Alves, E., Martins, G. A., Bourtsoukidis, E., Brito, J., Jardine, K., Artaxo, P., and Kesselmeier, J.: Diel and seasonal changes of biogenic volatile organic compounds within and above an Amazonian rainforest, Atmospheric Chemistry and Physics, 15, 3359–3378, https://doi.org/10.5194/acp-15-3359-2015, 2015.

Yáñez-Serrano, A. M., Bourtsoukidis, E., Alves, E. G., Bauwens, M., Stavrakou, T., Llusià, J., Filella, I., Guenther, A., Williams, J., Artaxo, P., Sindelarova, K., Doubalova, J., Kesselmeier, J., and Peñuelas, J.: Amazonian biogenic volatile organic compounds under global change, Global Change Biology, 26, 4722–4751, https://doi.org/10.1111/gcb.15185, 2020.

Zha, Q., Aliaga, D., Krejci, R., Sinclair, V. A., Wu, C., Ciarelli, G., Scholz, W., Heikkinen, L., Partoll, E., Gramlich, Y., Huang, W., Leiminger, M., Enroth, J., Peräkylä, O., Cai, R., Chen, X., Koenig, A. M., Velarde, F., Moreno, I., Petäjä, T.,

Artaxo, P., Laj, P., Hansel, A., Carbone, S., Kulmala, M., Andrade, M., Worsnop, D., Mohr, C., and Bianchi, F.: Oxidized organic molecules in the tropical free troposphere over Amazonia, Natl Sci Rev, 11, nwad138, https://doi.org/10.1093/nsr/nwad138, 2024.

Zha, Q., Aliaga, D., Krejci, R., Sinclair, V. A., Wu, C., Ciarelli, G., Scholz, W., Heikkinen, L., Partoll, E., Gramlich, Y., Huang, W., Leiminger, M., Enroth, J., Peräkylä, O., Cai, R., Chen, X., Koenig, A. M., Velarde, F., Moreno, I., Petäjä, T.,
Artaxo, P., Laj, P., Hansel, A., Carbone, S., Kulmala, M., Andrade, M., Worsnop, D., Mohr, C., and Bianchi, F.: Oxidized organic molecules in the tropical free troposphere over Amazonia, Natl Sci Rev, 11, nwad138, https://doi.org/10.1093/nsr/nwad138, 2024.

Zhao, B., Fast, J., Shrivastava, M., Donahue, N. M., Gao, Y., Shilling, J. E., Liu, Y., Zaveri, R. A., Gaudet, B., Wang, S., Wang, J., Li, Z., and Fan, J.: Formation Process of Particles and Cloud Condensation Nuclei Over the Amazon Rainforest: The Role of Local and Remote New-Particle Formation, Geophysical Research Letters, 49, e2022GL100940, https://doi.org/10.1029/2022GL100940, 2022.

Zhao, B., Donahue, N. M., Zhang, K., Mao, L., Shrivastava, M., Ma, P.-L., Shen, J., Wang, S., Sun, J., Gordon, H., Tang, S., Fast, J., Wang, M., Gao, Y., Yan, C., Singh, B., Li, Z., Huang, L., Lou, S., Lin, G., Wang, H., Jiang, J., Ding, A., Nie, W., Qi, X., Chi, X., and Wang, L.: Global variability in atmospheric new particle formation mechanisms, Nature, 631, 98–105, https://doi.org/10.1038/s41586-024-07547-1, 2024.